

---

# Adversarial Sample-Based Approach for Tighter Privacy Auditing in Final Model-Only Scenarios

---

**Sangyeon Yoon\***  
 Hongik University  
 B911117@g.hongik.ac.kr

**Wonje Jeung\***  
 Yonsei University  
 specific0924@yonsei.ac.kr

**Albert No**  
 Yonsei University  
 albertno@yonsei.ac.kr

## Abstract

Auditing Differentially Private Stochastic Gradient Descent (DP-SGD) in the final model setting is challenging and often results in empirical lower bounds that are significantly looser than theoretical privacy guarantees. We introduce a novel auditing method that achieves tighter empirical lower bounds without additional assumptions by crafting worst-case adversarial samples through loss-based input-space auditing. Our approach surpasses traditional canary-based heuristics and is effective in both white-box and black-box scenarios. Specifically, with a theoretical privacy budget of  $\epsilon = 10.0$ , our method achieves empirical lower bounds of 6.68 in white-box settings and 4.51 in black-box settings, compared to the baseline of 4.11 for MNIST. Moreover, we demonstrate that significant privacy auditing results can be achieved using in-distribution (ID) samples as canaries, obtaining an empirical lower bound of 4.33 where traditional methods produce near-zero leakage detection. Our work offers a practical framework for reliable and accurate privacy auditing in differentially private machine learning.

## 1 Introduction

Differentially Private Stochastic Gradient Descent (DP-SGD) [Abadi et al., 2016] was introduced to prevent sensitive information leakage from training data in models trained using Stochastic Gradient Descent (SGD) [Shokri et al., 2017, Hayes et al., 2017, Yeom et al., 2018, Bichsel et al., 2021, Balle et al., 2022, Haim et al., 2022, Carlini et al., 2022]. DP-SGD mitigates privacy leakage by clipping individual gradients and adding Gaussian noise to the aggregated gradient updates.

However, correctly implementing DP-SGD is challenging, and several implementations have revealed bugs that compromise its privacy guarantees [Ding et al., 2018, Bichsel et al., 2021, Stadler et al., 2022, Tramer et al., 2022]. These issues introduce potential privacy leakage, making thorough audits essential to ensure that privacy guarantees hold in practice. Audits commonly employ membership inference attacks (MIAs) [Shokri et al., 2017], using success rates to empirically estimate privacy leakage and compare it against theoretical upper bounds [Jagielski et al., 2020, Nasr et al., 2021, 2023]. If the empirical privacy leakage, represented by the lower bound on  $\epsilon$ , is significantly lower than the theoretical upper bound, the audit results are considered *loose*; conversely, when the lower bound closely approaches the upper bound, the results are regarded as *tight*. In *intermediate model* settings, where adversaries can observe gradients throughout the entire training process, previous works [Nasr et al., 2021, 2023] have shown that achieving tight privacy auditing is feasible. However,

---

\*These authors contributed equally.

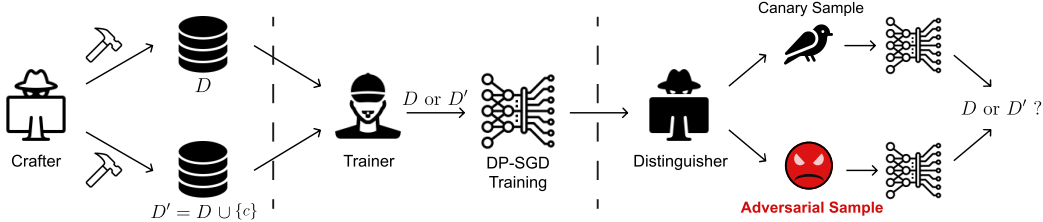


Figure 1: Overview of privacy auditing process. The Crafter crafts a canary and constructs two neighboring datasets,  $D$  and  $D'$ , where  $D'$  contains the canary. The Trainer trains a model on either  $D$  or  $D'$  using the DP-SGD. The Distinguisher observes the loss values for specific input to infer whether the model was trained on  $D$  or  $D'$ . We suggest an adversarial sample for *tighter* auditing.

this approach is often impractical, as real-world scenarios usually restrict adversaries’ access to only the final model. Achieving rigorous audit results in the *final model* settings remains challenging, leaving the feasibility of final model auditing for DP-SGD an unresolved issue.

To address these challenges, the final model setting has gained attention in practical applications as a promising method to improve the privacy-utility trade-off. By concealing intermediate steps and exposing only the final model, this approach aligns more closely with real-world constraints. Theoretically, in the final model setting, privacy amplification by iteration can provide additional privacy protection for data points involved in earlier stages of training [Feldman et al., 2018, Balle et al., 2019, Chourasia et al., 2021, Ye and Shokri, 2022, Altschuler and Talwar, 2022, Bok et al., 2024]. However, this effect has primarily been observed in convex or smooth loss functions, leaving its applicability to non-convex problems unresolved.

Building on this theoretical foundation, several works [Nasr et al., 2021, 2023, Andrew et al., 2023, Steinke et al., 2024b,a, Cebere et al., 2024] have explored privacy amplification in final model settings with non-convex loss functions. They observed a significant gap between empirical lower bounds and theoretical upper bounds, suggesting that privacy amplification by iteration may extend to general non-convex loss functions. However, there is no formal proof to support this, and the observed gap may instead reflect that adversaries have not fully exploited their potential capabilities.

Conversely, recent works [Annamalai, 2024, Cebere et al., 2024] have observed that privacy amplification does not occur in non-convex settings. These findings, however, apply only to specific cases, such as constructing a worst-case non-convex loss function for DP-SGD where information from all previous iterations is encoded in the final iteration, or manually designing a gradient sequence. These efforts remain constrained to additional assumptions or highly specific scenarios, leaving the broader question of whether privacy amplification can occur in general non-convex settings unresolved.

In this work, we introduce a novel auditing approach designed to establish tighter lower bounds in general non-convex settings for final model scenarios, without requiring any additional assumptions. Our method leverages loss-based input-space auditing to craft worst-case adversarial samples, enhancing the precision of privacy auditing results. Previous works [Jagielski et al., 2020, Nasr et al., 2021, Tramer et al., 2022, Aerni et al., 2024] on input-space auditing have implicitly assumed that the canary sample represents the worst-case privacy leakage, using it as an adversarial sample for MIAs based on its loss outputs. However, relying solely on canary-based approaches may not yield tighter empirical lower bounds. By leveraging loss outputs from an alternative adversarial sample, our approach identifies increased privacy leakage. Consequently, we craft worst-case adversarial samples without relying on canaries, providing tighter empirical lower bounds for auditing.

Our auditing method addresses practical challenges in two scenarios within the final model setting. First, for the *white-box auditing* scenario, adversaries have access to the final model’s weights, as in open-source cases. We craft the worst-case adversarial sample directly using these weights. For example, with a theoretical privacy budget of 10.0, our approach achieves an empirical lower bound of 6.68, significantly surpassing the 4.11 obtained with the canary approach. Secondly, for the *black-box auditing* scenario, only the model’s outputs are accessible, such as through APIs. We employ surrogate models to approximate the final models and use their weights to craft the worst-case adversarial sample. While adversaries’ capabilities are more limited in the black-box setting compared to the white-box setting, our approach increases the empirical lower bound from 4.11,

achieved using the canary approach, to 4.51 for a theoretical upper bound of 10.0. This demonstrates that our approach provides generalizable and effective privacy auditing results, even in scenarios with restricted adversarial access.

Additionally, we show that significant privacy auditing results can be achieved by using in-distribution (ID) samples from the training dataset as canaries, eliminating the need for out-of-distribution (OOD) samples. When an ID sample is used as the canary, the canary approach yields empirical privacy leakage close to zero, indicating little privacy leakage detection. In contrast, we achieve an empirical lower bound of 4.33 even with ID canaries.

## 2 Preliminary

**Differentially Private Training.** Differential Privacy (DP) [Dwork et al., 2006] is a widely used standard for preserving individual privacy in data analysis. A randomized mechanism  $\mathcal{M}$  is considered  $(\epsilon, \delta)$ -differentially private if, for any two neighboring datasets  $D$  and  $D'$  that differ by only one data point known as the **canary** ( $c$ ), and for any possible output subset  $O \subseteq \text{Range}(\mathcal{M})$ , the following inequality holds:

$$\Pr[\mathcal{M}(D) \in O] \leq e^\epsilon \Pr[\mathcal{M}(D') \in O] + \delta$$

In this formulation,  $\epsilon$  represents the loss of privacy, with smaller  $\epsilon$  indicating stronger privacy guarantees. The parameter  $\delta \in (0, 1)$  represents a small probability that the privacy guarantee may not hold.

Numerous mechanisms have been developed to ensure differential privacy during the training of machine learning models. [Abadi et al., 2016, Papernot et al., 2016, Zhu et al., 2020]. Differentially Private Stochastic Gradient Descent (DP-SGD) [Abadi et al., 2016] is widely used to achieve differential privacy. DP-SGD clips gradients to a maximum norm  $C$  to limit the impact of individual data points on model parameters, then adds Gaussian noise scaled by  $\sigma$  to ensure privacy across training steps. This mechanism allows DP-SGD to provide a theoretical upper bound on cumulative privacy loss, ensuring privacy throughout training (known as **privacy accounting**). The complete DP-SGD algorithm is shown in Algorithm 1.

---

### Algorithm 1 DP-SGD

---

```

1: Input: Training dataset  $D$ , Loss function  $\ell$ , Iterations  $T$ , Initial model parameters  $\theta_0$ , Learning rate  $\eta$ , Batch size  $B$ , Clipping norm  $C$ , Noise multiplier  $\sigma$ 
2: for  $t \in [T]$  do
3:   Sample  $L_t$  from  $D$  using poisson sampling with
4:   probability  $B/|D|$ 
5:   for  $x_i \in L_t$  do
6:      $g_t(x_i) \leftarrow \nabla_{\theta_t} \ell(\theta_t; x_i)$ 
7:      $\bar{g}_t(x_i) \leftarrow g_t(x_i) / \max(1, \frac{\|g_t(x_i)\|_2}{C})$ 
8:      $\tilde{g}_t \leftarrow \frac{1}{B} (\sum_i \bar{g}_t(x_i) + \mathcal{N}(0, (C\sigma)^2 \mathbb{I}))$ 
9:      $\theta_{t+1} \leftarrow \theta_t - \eta \tilde{g}_t$ 
10:  return  $\theta_T$ 

```

---

**Privacy Auditing.** Although DP-SGD provides a theoretical upper bound on privacy budgets  $(\epsilon, \delta)$ , relying solely on privacy accounting poses challenges. First, Theoretical analyses, while crucial, are demonstrated to be conservative [Bassily et al., 2014, Kairouz et al., 2015, Abadi et al., 2016, Mironov, 2017, Koskela et al., 2020, Gopi et al., 2021, Doroshenko et al., 2022], which can lead to overestimating the required noise and subsequently reducing the utility of the model [Nasr et al., 2021]. Second, the complexity of DP-SGD training can lead to implementation errors that compromise privacy guarantees [Ding et al., 2018, Tramer et al., 2022]. Privacy auditing addresses these issues by establishing empirical lower bounds on privacy, providing a more realistic assessment of privacy loss.

In privacy auditing, Nasr et al. [2021] decomposes the attack process into three main components: **Crafter**, **Trainer**, and **Distinguisher**. The Crafter generates a canary sample  $c$  to distinguish between neighboring datasets  $D$  and  $D'$  (*i.e.*,  $D' = D \cup \{c\}$ ). The Trainer then trains a model on one of these two datasets using the DP-SGD training algorithm. Finally, the Distinguisher receives the datasets  $D$

and  $D'$  from the Crafter, along with the trained model as input. The distinguisher then infers which dataset was used, with the accuracy of this inference indicating the level of privacy leakage. Together, the Crafter and the Distinguisher form the **adversary** ( $\mathcal{A}$ ).

**Privacy Auditing Setup.** Privacy auditing can be categorized into two settings based on adversaries' access levels: intermediate models [Nasr et al., 2021, 2023, Andrew et al., 2023, Steinke et al., 2024b, Mahloujifar et al., 2024], final model [Jagielski et al., 2020, Nasr et al., 2021, Annamalai and De Cristofaro, 2024, Cebere et al., 2024, Steinke et al., 2024a]. For the **intermediate models** setup, the adversaries have full access to the model parameters during all training steps. Previous works [Nasr et al., 2021, 2023] have demonstrated that privacy auditing in this setup achieves a *tight* lower bound, where the theoretical upper bound and the empirical lower bound ( $\varepsilon_{emp}$ ) can align.

However, in practice, adversaries are more likely to have access only to the **final model** rather than to all intermediate training steps. Access to the final model is available either through its outputs, such as via APIs, or through direct access to its weights, as in open-source models. In the case of access to the final model through an API, a substantial gap remains between  $\varepsilon$  and  $\varepsilon_{emp}$ . Although Annamalai and De Cristofaro [2024] attempts to address this, their approach requires additional assumptions on initialized parameters and still lacks tightness. In contrast, recent works [Annamalai, 2024, Cebere et al., 2024] aim for tight auditing via direct access to model weights in the final model setting. However, their auditing methods focus on specific scenarios, such as constructing worst-case non-convex loss functions for DP-SGD, manually designing gradient sequences, or assuming access to the initial parameters ( $\theta_0$ ). Our work delivers tighter privacy auditing **without additional assumptions**, relying solely on final model.

Privacy auditing techniques can be broadly classified into gradient-space auditing and input-space auditing, based on the modifications allowed by the Crafter. In gradient-space auditing [Nasr et al., 2021, Maddock et al., 2022, Nasr et al., 2023, Andrew et al., 2023, Steinke et al., 2024b], the gradient canary is embedded directly into the gradients during training, allowing targeted gradient-level interventions. In contrast, input space auditing [Jagielski et al., 2020, Zanella-Beguelin et al., 2023, Andrew et al., 2023, Steinke et al., 2024a] uses a canary in the form of an input sample, focusing on the training data itself. In our experiments, we adopt input-space auditing, which is more practical.

### 3 DP-SGD Auditing procedure

Recent privacy auditing studies [Nasr et al., 2021, Tramer et al., 2022, Nasr et al., 2023, Steinke et al., 2024a, Cebere et al., 2024, Chadha et al., 2024] often employ membership inference attacks (MIAs) [Shokri et al., 2017] to determine whether a specific sample was included in the training data by analyzing the outputs of  $\mathcal{M}(D)$  or  $\mathcal{M}(D')$ . Similarly, our auditing procedure in Algorithm 2 uses MIAs to evaluate the privacy guarantees of the model, consistent with their widespread adoption as the de facto standard in many privacy studies [Jeon et al., 2024, Thaker et al., 2024].

The procedure begins with Crafter phase. A canary Crafter crafts a canary sample  $c$  as an outlier within the training dataset  $D$ . This canary sample is then inserted into the original dataset to create a neighboring dataset,  $D' = D \cup \{c\}$ . In our experiments, following prior works [De et al., 2022, Nasr et al., 2023, Steinke et al., 2024a], we primarily use a blank image as the canary to maximize its distinctiveness from typical training samples.

In the **Model Trainer** phase, trainer applies the DP-SGD mechanism  $\mathcal{M}$  to both  $D$  and  $D'$ , producing  $N$  models for each dataset, denoted as  $\{M_i\}_{i=1}^N$  and  $\{M'_i\}_{i=1}^N$ , respectively. These models are trained independently to analyze the effect of canary insertion across multiple models.

The **Distinguisher** phase performs the core auditing process. It first crafts an adversarial sample  $a$ , then computes the loss values of this sample across all models, forming output sets  $O$  and  $O'$  for  $\{M_i\}_{i=1}^N$  and  $\{M'_i\}_{i=1}^N$ , respectively. Using a decision threshold  $\tau$  determined by a separate dataset (e.g., a validation set), the Distinguisher calculates the False Positive Rate (FPR) and False Negative Rate (FNR) based on  $O$  and  $O'$ . It then computes the upper bounds of FPR and FNR using Clopper-Pearson confidence intervals [Clopper and Pearson, 1934]. Finally, based on the empirical upper bounds FPR and FNR, the Distinguisher estimates the empirical lower bound for the privacy parameter  $\varepsilon$  at a given  $\delta$ , denoted as  $\varepsilon_{emp}$ .

---

**Algorithm 2** Auditing Procedure

---

```

1: Input: Training dataset  $D$ , DP-SGD mechanism  $\mathcal{M}$ , Loss function  $\ell$ , Number of observations  $N$ , Decision threshold  $\tau$ , Confidence level  $\alpha$ , Privacy parameter  $\delta$ 
2: Initialize observations  $O, O'$ 
3: Craft Canary sample  $c$ 
4:  $D' \leftarrow D \cup \{c\}$ 
5: for  $i \in [N]$  do
6:    $M_i \leftarrow \mathcal{M}(D)$ 
7:    $M'_i \leftarrow \mathcal{M}(D')$ 
8: Craft Adversarial sample  $a$ 
9: for  $i \in [N]$  do
10:   $O[i] \leftarrow \ell(M_i; a)$ 
11:   $O'[i] \leftarrow \ell(M'_i; a)$ 
12:  $\text{FPR} \leftarrow \frac{1}{N} \sum_{o \in O} \mathbb{I}(o \geq \tau)$ 
13:  $\text{FNR} \leftarrow \frac{1}{N} \sum_{o \in O'} \mathbb{I}(o < \tau)$ 
14:  $\overline{\text{FPR}} \leftarrow \text{Clopper-Pearson}(\text{FPR}, N, \alpha)$ 
15:  $\overline{\text{FNR}} \leftarrow \text{Clopper-Pearson}(\text{FNR}, N, \alpha)$ 
16:  $\varepsilon_{\text{emp}} \leftarrow \text{EstimateDP}(\text{FPR}, \overline{\text{FNR}}, \delta)$ 
17: return  $\varepsilon_{\text{emp}}$ 

```

---

Nasr et al. [2023] demonstrated that the privacy region for DP-SGD aligns more closely with the  $\mu$ -Gaussian Differential Privacy guarantee ( $\mu$ -GDP) [Dong et al., 2022] than with the  $(\varepsilon, \delta)$ -DP guarantee, establishing a direct relationship between  $\overline{\text{FPR}}$ ,  $\overline{\text{FNR}}$ , and  $\mu$ . Furthermore, it enables a tighter estimate of privacy leakage with fewer training runs than  $(\varepsilon, \delta)$ -DP. In addition, when deciding the decision threshold, any value for  $\mu$ -GDP has an equal likelihood of maximizing the lower bound given a sufficient number of observations [Nasr et al., 2023]. Following previous work [Nasr et al., 2021, Maddock et al., 2022, Zanella-Beguelin et al., 2023], we use the threshold that maximizes the  $\varepsilon$  lower bound for the same set of observations.

Calculating a empirical bound for  $\mu$  in  $\mu$ -GDP, which can be converted to a lower bound for  $\varepsilon$  in  $(\varepsilon, \delta)$ -DP, provides an effective estimate of privacy leakage. To compute a lower bound on the privacy parameters of the Gaussian mechanism (i.e.,  $\mu$ ), we have:

$$\mu_{\text{emp}} = \Phi^{-1}(1 - \overline{\text{FPR}}) - \Phi^{-1}(\overline{\text{FNR}}),$$

where  $\Phi^{-1}$  is the inverse of the standard normal CDF. Then,  $\mu_{\text{emp}}$  corresponds to  $\varepsilon_{\text{emp}}$  by following Corollary.

**Corollary 1** ( $\mu$ -GDP to  $(\varepsilon, \delta)$ -DP conversion [Dong et al., 2022]). *A mechanism is  $\mu$ -GDP if and only if it is  $(\varepsilon, \delta(\varepsilon))$ -DP for all  $\varepsilon \geq 0$ , where:*

$$\delta(\varepsilon) = \Phi\left(-\frac{\varepsilon}{\mu} + \frac{\mu}{2}\right) - e^\varepsilon \Phi\left(-\frac{\varepsilon}{\mu} - \frac{\mu}{2}\right).$$

$\Phi$  is the standard normal CDF.

We apply this  $\mu$ -GDP based auditing scheme with  $\delta = 10^{-5}$  across all experiments.

## 4 Crafting Adversarial Samples for Tighter Privacy Auditing

To obtain tighter lower bounds for membership inference attacks (MIAs), some studies [Nasr et al., 2021, 2023] craft input canaries based on the final model weights during line 3 of Algorithm 2. In contrast, most prior works [Carlini et al., 2019, Jagielski et al., 2020, Nasr et al., 2021, Aerni et al., 2024, Annamalai and De Cristofaro, 2024] rely on the heuristic assumption that the most vulnerable data point serves as the canary sample in the line 8 of the same algorithm. In our study, instead of relying on a canary-based approach, we directly construct the worst-case adversarial sample, adhering to the requirement that every output must satisfy the differential privacy guarantee, thereby ensuring fundamental indistinguishability across all possible input samples. To the best of our knowledge, this is the first attempt in loss-based input-space auditing to achieve tighter lower bounds by using a worst-case adversarial sample instead of a traditional canary.

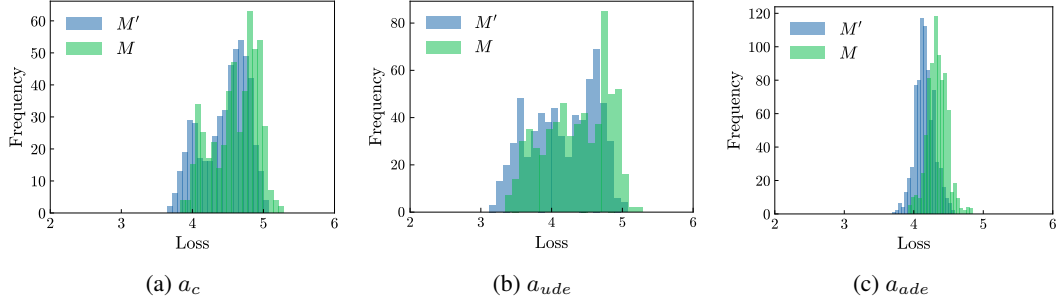


Figure 2: The loss distributions of three adversarial samples ( $a_c, a_{ude}, a_{ade}$ ) at a fixed privacy budget  $\varepsilon = 10.0$ . The green distribution represents the loss outputs of models  $M$ , while the blue distribution represents the loss outputs of models  $M'$ .

To enable tighter privacy auditing, we craft a worst-case adversarial sample  $a_w$  that maximizes the distinguishable difference between the distributions of outputs  $O$  and  $O'$ . This involves designing a specialized loss function to enhance the separability of these distributions. When crafting  $a_w$ , we leverage the Distinguisher's knowledge of the canary by initializing the adversarial sample  $a = (x_a, y_a)$  with the canary's values  $c = (x_c, y_c)$ . Each pixel of  $x_a$  is treated as an learnable variable to form the worst-case scenario, while the label  $y_a$  is fixed as a constant  $y_c$ .

Our initial loss function,  $\mathcal{L}_{ude}$  (Uniform Distance Expansion), is based on the observation that the canary's loss is naturally higher in models trained on dataset  $D$  (denoted as  $M_i$ ) than in models trained on  $D'$  (denoted as  $M'_i$ ). Therefore, we train the adversarial sample to ensure that models  $M_i$  produce a higher loss and models  $M'_i$  produce a lower loss when evaluating  $a_w$ , aiming to maximize the distinguishability between their output distributions. The loss function  $\mathcal{L}_{ude}$  is defined as:

$$\mathcal{L}_{ude}(x_a) = \frac{1}{N} \sum_{i=1}^N (\ell(M'_i(x_a), y_a) - \ell(M_i(x_a), y_a)),$$

and the corresponding minimizer,  $a_{ude}$ . However, as illustrated in Figure 2b, using  $\mathcal{L}_{ude}$  can lead to unnecessary training on the non-overlapping regions of the two distributions. This results in increased dispersion rather than improved separation between the distributions.

To address this issue, we propose an adaptive loss function  $\mathcal{L}_{ade}$  (Adaptive Distance Expansion) that focuses solely on the overlapping regions of the loss distributions, avoiding training on already distinguishable values. This targeted approach improves the distinction between the distributions, as depicted in Figure 2c. The adaptive loss function  $\mathcal{L}_{ade}$  is defined as:

$$\mathcal{L}_{ade}(x_a) = \frac{1}{N} \sum_{i=1}^N \text{ReLU} \left( \ell(M'_i(x_a), y_a) - \frac{1}{N} \sum_{j=1}^N \ell(M_j(x_a), y_a) + \alpha \right),$$

and the corresponding minimizer,  $a_{ade}$ .

In this equation,  $\mathcal{L}_{ade}$  adjusts the loss based on how much each  $M'_i$  loss deviates from the mean loss of all models  $M_j$ . The function ReLU ensures that only positive deviations contribute to the loss, effectively limiting unnecessary updates when  $M'_i$  loss is already sufficiently separated from the mean. This allows the training process to focus on further separating less distinct distributions. Here,  $\alpha$  is a tunable margin that controls the sensitivity of the separation adjustment. Increasing  $\alpha$  seeks to further separate the distributions but may risk isolating only a few samples. In this work, we set  $\alpha = 0.2$  for all experiments. Further analysis of the impact of  $\alpha$  is provided in Section 5.4.

## 5 Experiments

### 5.1 Experiments Setup

To evaluate our auditing procedure, we conduct experiments on MNIST [LeCun et al., 1998] and CIFAR-10 [Krizhevsky, 2009] datasets with ConvNet models. We use ConvNet following the work

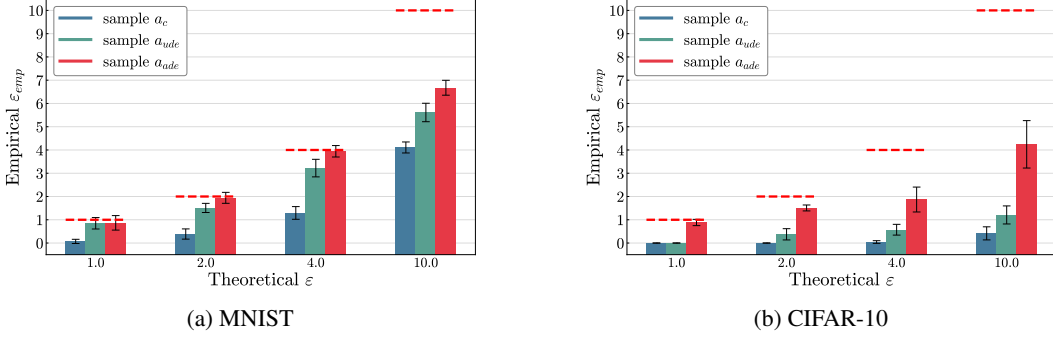


Figure 3: *White-box* privacy auditing results on MNIST and CIFAR-10 datasets, comparing three adversarial samples:  $a_c$ ,  $a_{ude}$ , and  $a_{aude}$ , across privacy budgets  $\varepsilon \in \{1.0, 2.0, 4.0, 10.0\}$ .

of Annamalai and De Cristofaro [2024]. We set the learning rate to  $\eta = 4$  for MNIST and  $\eta = 2$  for CIFAR-10. The training process runs for  $T = 100$  iterations on MNIST and  $T = 200$  iterations on CIFAR-10.

For models trained with DP-SGD, the accuracy on MNIST is nearly 95% for all  $\varepsilon$ , while the accuracy on CIFAR-10 is around 52% at  $\varepsilon = 10.0$ . This is due to the fact that models on CIFAR-10 converge much more slowly [Annamalai and De Cristofaro, 2024]; however, increasing the number of training epochs can raise the accuracy to around 70%, making it comparable to the state-of-the-art [De et al., 2022].

**Implementation Details.** To ensure robustness, we perform 10 independent runs for each experiment and report the average value of  $\varepsilon_{\text{emp}}$  along with its standard deviation, and the theoretical upper bound for  $\varepsilon$  is computed using the privacy accountant provided by Opacus [Yousefpour et al., 2021]. In each run, we generate  $2N = 256$  models—128 with canary ( $M'$ ) and 128 without canary ( $M$ ). We compute empirical lower bounds using the  $\mu$ -GDP approach, following previous works [Nasr et al., 2023, Cebere et al., 2024], and report the lower bounds with 95% confidence intervals.

Additionally, to simplify the privacy analysis, we set the sampling rate to 1, performing DP-SGD with full-batch training ( $B = |D|$ ). While, analyzing DP-SGD with both subsampling amplification and multi-step composition is challenging, and relying on the central limit theorem for subsampling may underestimate the privacy budget due to the emergence of mixture distributions [Nasr et al., 2023]. Although the Privacy Loss Distribution (PLD) [Koskela et al., 2020] is used to approximate the trade-off function and address this issue [Nasr et al., 2023], PLD lacks a closed-form trade-off function and provides a looser bound for  $\varepsilon$ . For these reasons, we focus our analysis on the full-batch setting.

## 5.2 White-Box Auditing in Final Model

In Figure 3, we compare the empirical privacy bounds  $\varepsilon_{\text{emp}}$  between the canary sample ( $a_c$ ) and our crafted worst-case samples ( $a_w$ ). For  $a_c$ , we use the default canary that differentiates  $D$  and  $D'$ . For  $a_w$ , we employ samples generated using the loss functions  $\mathcal{L}_{ude}$  and  $\mathcal{L}_{aude}$ , resulting in  $a_{ude}$  and  $a_{aude}$ , respectively. Utilizing  $a_w$  for privacy auditing consistently yields tighter empirical lower bounds across various theoretical upper bounds compared to the baseline  $a_c$ . For instance, with a theoretical privacy budget of  $\varepsilon = 10.0$ , a canary sample  $a_c$  produces empirical lower bounds of 4.11 for MNIST and 0.30 for CIFAR-10. In contrast,  $a_{ude}$  and  $a_{aude}$  yield estimates of 5.61 and 6.68 for MNIST, and 1.05 and 4.10 for CIFAR-10, respectively. Notably, when using  $a_c$  on CIFAR-10, we observe almost no detectable privacy leakage. However, employing  $a_{aude}$  reveals significant privacy leakage. This demonstrates  $a_{aude}$ 's superior effectiveness in providing tighter empirical lower bounds on privacy.

## 5.3 Black-box Auditing in Final Model

We also conduct privacy auditing in the final model setting when the Distinguisher has access only to the model output. In this setting, since the Distinguisher cannot directly access the weights of the final model, it is not feasible to directly train adversarial sample through final model. Instead, leveraging the fact that the Distinguisher knows both neighboring datasets  $D$  and  $D'$ , we apply distillation

techniques to train 128 surrogate models using the output of  $D'$  for each model  $M$  and  $M'$ , resulting in a total of  $2N = 256$  models. These surrogate models, distilled from the final model output in  $D'$ , serve as proxies for  $M$  and  $M'$  ( $M_{sur}$  and  $M'_{sur}$ ). We then train the adversarial sample using  $M_{sur}$  and  $M'_{sur}$  going through the same process as white-box auditing.

As shown in Figure 4, although black-box auditing provides less tight results than white-box auditing due to the attacker’s limited access, the  $a_w$  trained by surrogate models consistently yields tighter lower bounds compared to the baseline  $a_c = c$ . Specifically, when the theoretical upper bound is 10.0, the empirical lower bound using the baseline  $a_c$  was 4.11, but it increased to 4.40 with  $a_{ude}$  and 4.51 with  $a_{ade}$ . Furthermore, while  $a_{ade}$  provided significantly tighter auditing results than  $a_{ude}$  in all privacy budgets in white-box auditing, both methods show similar lower bounds in black-box auditing. Since black-box auditing is typically limited to training interventions, crafting adversarial samples offers a promising approach for differential privacy auditing.

#### 5.4 Additional Results

**Canary type.** Typically, the canary sample used exclusively for training  $M'$  is an out-of-distribution (OOD) sample that differs significantly from the training dataset  $D$ . Without an OOD canary, obtaining tighter lower bounds becomes challenging, as the difference between  $M$  and  $M'$  is minimal. However, leveraging a worst-case adversarial sample enables significantly tighter lower bounds, even when using in-distribution (ID) canary.

As shown in Figure 5, audits using a standard ID canary sample yield zero empirical privacy leakage estimates ( $\varepsilon_{emp}$ ) across all privacy budgets when applying the baseline attack  $a_c$ . In contrast, adversarial samples improve auditing performance significantly. At  $\varepsilon = 10.0$ , the empirical lower bounds rise to 4.05 for  $a_{ude}$  and 4.33 for  $a_{ade}$ , demonstrating the effectiveness of  $a_w$  in exposing privacy leakage. Furthermore,  $a_{ade}$  consistently achieves slightly tighter bounds than  $a_{ude}$  across all privacy budgets, highlighting the robustness of adaptive attacks in privacy auditing. These results emphasize the importance of leveraging adversarial sample when auditing with ID canary.

Additionally, adversarial samples are effective across diverse canary types, including ID samples, blank samples, mislabeled samples and a clip-bkd samples. The mislabeled image is an OOD sample intentionally assigned the wrong label, and the clip-bkd image, crafted as proposed by Jagielski et al. [2020], target the direction of least variance to create a robust attack against the gradient clipping norm.

As shown in Figure 6,  $a_{ade}$  consistently achieves tighter lower bounds compared to the baseline ( $a_c$ ) across all canary types. Specifically, for ID canary, blank image, mislabeled image, and clip-bkd image, our method achieves  $\varepsilon_{emp} = 3.03, 3.94, 3.96$ , and  $3.91$ , respectively, significantly outperforming the baseline values of  $\varepsilon_{emp} = 0.00, 1.29, 0.93$ , and  $1.56$ . These results highlight the robustness of our approach in privacy auditing, demonstrating its effectiveness across ID and OOD canary.

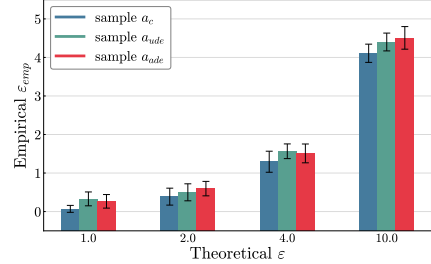


Figure 4: *Black-box* privacy auditing results on the MNIST dataset, comparing three auditing samples: the canary sample,  $a_{ude}$ , and  $a_{ade}$ , across privacy budgets  $\varepsilon \in \{1.0, 2.0, 4.0, 10.0\}$ .

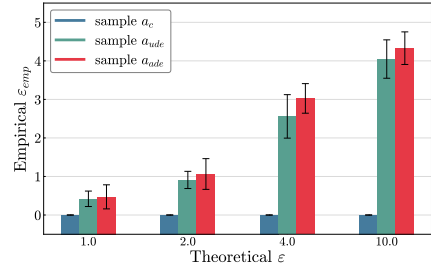


Figure 5: *White-box* privacy auditing results on the MNIST dataset when ordinary data is used as the canary sample, evaluated at privacy budgets  $\varepsilon \in \{1.0, 2.0, 4.0, 10.0\}$ . The adversarial sample successfully audits the model, while the default canary fails.

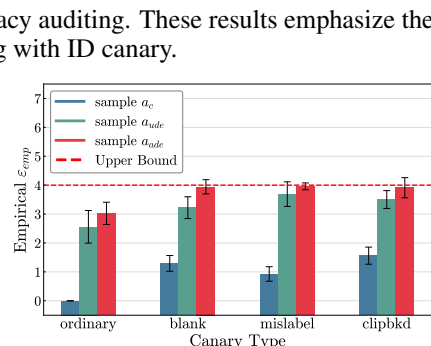


Figure 6: Privacy auditing results on the MNIST dataset using both in-distribution (ID) and out-of-distribution (OOD) data as the canary samples (blank, mislabel, clip-bkd), evaluated at a privacy budget of  $\varepsilon = 10.0$ .

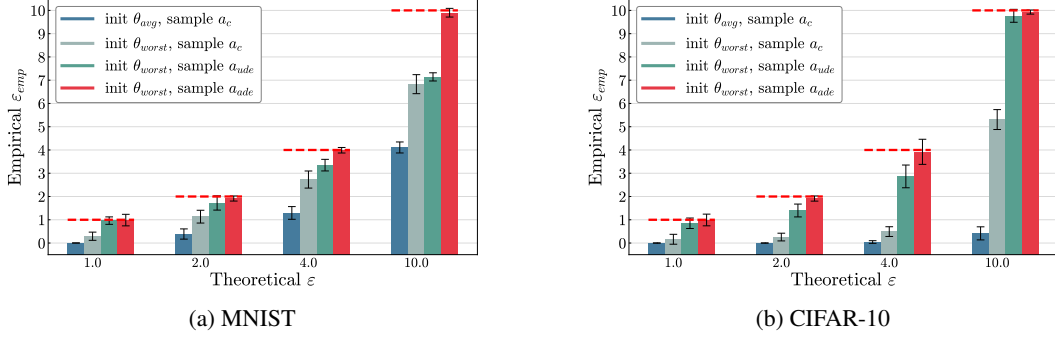


Figure 7: Privacy auditing results on the MNIST and CIFAR-10 datasets using *worst-case initialization* with adversarial sample, evaluated across privacy budgets  $\epsilon \in \{1.0, 2.0, 4.0, 10.0\}$ .

**Worst case initialization.** Recent work [Annamalai and De Cristofaro, 2024] leverages the insight that minimizing the gradients of non-canary samples enables tight auditing in DP-SGD, aiming to achieve this in black-box auditing of the final model by pre-training on an auxiliary dataset matching the training data distribution. These crafted worst-case initial model parameters are then used as the model’s initial weights, replacing random initialization to obtain tighter lower bounds in a black-box setting in final model.

In this section, we present our results on tighter privacy auditing for the final model trained on MNIST and CIFAR-10 datasets by combining the worst-case model parameters ( $\theta_{\text{worst}}$ ) with a worst-case adversarial sample ( $a_w$ ). As illustrated in Figure 7, using the canonical attack  $a_c$  with the average model parameters  $\theta_{\text{avg}}$  yielded lower bounds of 4.11 on MNIST and 0.41 on CIFAR-10. When we switched to the worst-case model parameters  $\theta_{\text{worst}}$  while using the same attack  $a_c$ , these lower bounds increased to 6.83 and 5.31, respectively, indicating tighter estimates of privacy leakage. Further improvements were achieved by employing the adaptive attack  $a_{\text{ade}}$  with  $\theta_{\text{worst}}$ , which resulted in even higher lower bounds of 9.9 on MNIST and 9.93 on CIFAR-10. Notably, across all theoretical privacy budgets, the auditing results using  $\theta_{\text{worst}}$  with  $a_{\text{ade}}$  closely aligned with the theoretical upper bounds. These findings demonstrate that we achieved tight privacy auditing, reinforcing the argument that privacy amplification in the final model setting does not occur with general non-convex loss.

**Clipping norm sensitivity.** Based on the experimental results, we analyze the impact of varying gradient clipping norms on the empirical privacy leakage estimates ( $\epsilon_{\text{emp}}$ ). Figure 8 presents the outcomes for three attack scenarios:  $a_c$ ,  $a_{\text{ude}}$ , and  $a_{\text{ade}}$ .

When the gradient clipping norm is small ( $C = 0.1$ ), the privacy leakage estimates are 5.90, 7.81 and 7.85 for  $a_c$ ,  $a_{\text{ude}}$  and  $a_{\text{ade}}$ , respectively, indicating tight audits due to a high signal-to-noise ratio. As the clipping norm increases to  $C = 1.0$ ,  $\epsilon_{\text{emp}}$  decreases across all scenarios; however, the rate of decrease varies. Notably,  $a_{\text{ade}}$  is less affected compared to  $a_c$  and  $a_{\text{ude}}$ , retaining a relatively high estimate of 4.24. This suggests that  $a_{\text{ade}}$  is more robust and capable of effectively auditing privacy leakage even with larger clipping norms. At a higher clipping norm ( $C = 10.0$ ),  $\epsilon_{\text{emp}}$  decreases significantly for all attacks, with values of 0.00, 0.59, and 0.87 for  $a_c$ ,  $a_{\text{ude}}$ , and  $a_{\text{ade}}$ , respectively. This reduction is attributed to excessive noise overwhelming the useful signal, resulting in looser audits.

These results highlight the trade-offs between gradient clipping norms and the tightness of privacy audits, emphasizing that adaptive attacks like  $a_{\text{ade}}$  can provide more effective auditing even under higher clipping norms.

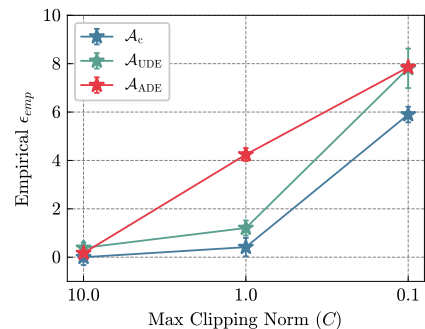


Figure 8: Auditing models trained with varying gradient clipping norms  $C$ , evaluated at privacy budgets  $\epsilon = 10.0$ .

Table 1: Privacy auditing results on the CIFAR-10 dataset for various values of  $\alpha$  with a theoretical privacy budget of  $\epsilon = 4.0$ .

$\alpha$	0.05	0.1	0.15	0.2	0.25
$\epsilon_{\text{emp}}$	$1.90 \pm 0.51$	$1.84 \pm 0.32$	$1.83 \pm 0.34$	$1.87 \pm 0.21$	$2.03 \pm 0.24$

$\alpha$  **sensitivity.** Although the worst-case adversarial sample demonstrates tighter privacy auditing performance, it relies on selecting an appropriate value for the hyperparameter  $\alpha$ . To assess the effect of  $\alpha$ , we trained adversarial samples using the  $\mathcal{L}_{ade}$  with  $\alpha$  set to various values: 0.05, 0.1, 0.15, 0.2, and 0.25. As shown in Table 1, the  $\mathcal{L}_{ade}$  exhibits similar auditing performance across these values, indicating that our loss function is robust to the choice of  $\alpha$ , which is advantageous. Empirically, we find that  $\alpha$  values between 0.02 and 0.5 do not result in significant performance degradation.

## 6 Conclusion

We introduce a novel method for crafting worst-case adversarial samples to achieve tighter lower bounds in privacy auditing of differentially private models, focusing on the final model setting. Unlike traditional canary-based approaches, our technique maximizes the distinguishability between output distributions by designing specialized loss functions, particularly the adaptive loss function  $\mathcal{L}_{ade}$ . This approach enhances the separability of overlapping regions in the loss distributions, leading to more effective auditing even when only the final model is accessible.

Our experiments on MNIST and CIFAR-10 datasets demonstrate that our method consistently provides tighter empirical lower bounds on privacy leakage compared to baseline methods, both in white-box and black-box settings. For instance, on CIFAR-10 with a theoretical privacy budget of  $\varepsilon = 10.0$ , the traditional canary-based method yields an empirical lower bound of only 0.30, whereas our approach achieves a significantly tighter lower bound of 4.10. Notably, our approach is effective even when using in-distribution (ID) samples as canaries, eliminating the need for out-of-distribution (OOD) samples. This robustness across various canary types highlights the practical applicability of our method.

By enabling more precise privacy auditing without relying on specific canary samples or additional assumptions, our work significantly advances the evaluation of differential privacy guarantees in the final model setting.

## References

Martin Abadi, Andy Chu, Ian Goodfellow, H Brendan McMahan, Ilya Mironov, Kunal Talwar, and Li Zhang. Deep learning with differential privacy. In *Proceedings of the 2016 ACM SIGSAC conference on computer and communications security*, pages 308–318, 2016.

Michael Aerni, Jie Zhang, and Florian Tramèr. Evaluations of machine learning privacy defenses are misleading. *arXiv preprint arXiv:2404.17399*, 2024.

Jason Altschuler and Kunal Talwar. Privacy of noisy stochastic gradient descent: More iterations without more privacy loss. *Advances in Neural Information Processing Systems*, 35:3788–3800, 2022.

Galen Andrew, Peter Kairouz, Sewoong Oh, Alina Oprea, H Brendan McMahan, and Vinith Suriyakumar. One-shot empirical privacy estimation for federated learning. *arXiv preprint arXiv:2302.03098*, 2023.

Meenatchi Sundaram Muthu Selva Annamalai. It’s our loss: No privacy amplification for hidden state dp-sgd with non-convex loss. *arXiv preprint arXiv:2407.06496*, 2024.

Meenatchi Sundaram Muthu Selva Annamalai and Emiliano De Cristofaro. Nearly tight black-box auditing of differentially private machine learning. *arXiv preprint arXiv:2405.14106*, 2024.

Borja Balle, Gilles Barthe, Marco Gaboardi, and Joseph Geumlek. Privacy amplification by mixing and diffusion mechanisms. *Advances in neural information processing systems*, 32, 2019.

Borja Balle, Giovanni Cherubin, and Jamie Hayes. Reconstructing training data with informed adversaries. In *2022 IEEE Symposium on Security and Privacy (SP)*, pages 1138–1156. IEEE, 2022.

Raef Bassily, Adam Smith, and Abhradeep Thakurta. Private empirical risk minimization: Efficient algorithms and tight error bounds. In *2014 IEEE 55th annual symposium on foundations of computer science*, pages 464–473. IEEE, 2014.

Benjamin Bichsel, Samuel Steffen, Ilija Bogunovic, and Martin Vechev. Dp-sniper: Black-box discovery of differential privacy violations using classifiers. In *2021 IEEE Symposium on Security and Privacy (SP)*, pages 391–409. IEEE, 2021.

Jinho Bok, Weijie Su, and Jason M Altschuler. Shifted interpolation for differential privacy. *arXiv preprint arXiv:2403.00278*, 2024.

Nicholas Carlini, Chang Liu, Úlfar Erlingsson, Jernej Kos, and Dawn Song. The secret sharer: Evaluating and testing unintended memorization in neural networks. In *28th USENIX security symposium (USENIX security 19)*, pages 267–284, 2019.

Nicholas Carlini, Steve Chien, Milad Nasr, Shuang Song, Andreas Terzis, and Florian Tramer. Membership inference attacks from first principles. In *2022 IEEE Symposium on Security and Privacy (SP)*, pages 1897–1914. IEEE, 2022.

Tudor Cebere, Aurélien Bellet, and Nicolas Papernot. Tighter privacy auditing of dp-sgd in the hidden state threat model. *arXiv preprint arXiv:2405.14457*, 2024.

Karan Chadha, Matthew Jagielski, Nicolas Papernot, Christopher Choquette-Choo, and Milad Nasr. Auditing private prediction. *arXiv preprint arXiv:2402.09403*, 2024.

Rishav Chourasia, Jiayuan Ye, and Reza Shokri. Differential privacy dynamics of langevin diffusion and noisy gradient descent. *Advances in Neural Information Processing Systems*, 34:14771–14781, 2021.

Charles J Clopper and Egon S Pearson. The use of confidence or fiducial limits illustrated in the case of the binomial. *Biometrika*, 26(4):404–413, 1934.

Soham De, Leonard Berrada, Jamie Hayes, Samuel L Smith, and Borja Balle. Unlocking high-accuracy differentially private image classification through scale. *arXiv preprint arXiv:2204.13650*, 2022.

Zeyu Ding, Yuxin Wang, Guanhong Wang, Danfeng Zhang, and Daniel Kifer. Detecting violations of differential privacy. In *Proceedings of the 2018 ACM SIGSAC Conference on Computer and Communications Security*, pages 475–489, 2018.

Jinshuo Dong, Aaron Roth, and Weijie J Su. Gaussian differential privacy. *Journal of the Royal Statistical Society: Series B (Statistical Methodology)*, 84(1):3–37, 2022.

Vadym Doroshenko, Badih Ghazi, Pritish Kamath, Ravi Kumar, and Pasin Manurangsi. Connect the dots: Tighter discrete approximations of privacy loss distributions. *arXiv preprint arXiv:2207.04380*, 2022.

Cynthia Dwork, Frank McSherry, Kobbi Nissim, and Adam Smith. Calibrating noise to sensitivity in private data analysis. In *Theory of Cryptography: Third Theory of Cryptography Conference, TCC 2006, New York, NY, USA, March 4-7, 2006. Proceedings* 3, pages 265–284. Springer, 2006.

Vitaly Feldman, Ilya Mironov, Kunal Talwar, and Abhradeep Thakurta. Privacy amplification by iteration. In *2018 IEEE 59th Annual Symposium on Foundations of Computer Science (FOCS)*, pages 521–532. IEEE, 2018.

Sivakanth Gopi, Yin Tat Lee, and Lukas Wutschitz. Numerical composition of differential privacy. *Advances in Neural Information Processing Systems*, 34:11631–11642, 2021.

Niv Haim, Gal Vardi, Gilad Yehudai, Ohad Shamir, and Michal Irani. Reconstructing training data from trained neural networks. *Advances in Neural Information Processing Systems*, 35: 22911–22924, 2022.

Jamie Hayes, Luca Melis, George Danezis, and Emiliano De Cristofaro. Logan: Membership inference attacks against generative models. *arXiv preprint arXiv:1705.07663*, 2017.

Matthew Jagielski, Jonathan Ullman, and Alina Oprea. Auditing differentially private machine learning: How private is private sgd? *Advances in Neural Information Processing Systems*, 33: 22205–22216, 2020.

Dongjae Jeon, Wonje Jeung, Taeheon Kim, Albert No, and Jonghyun Choi. An information theoretic metric for evaluating unlearning models. *arXiv preprint arXiv:2405.17878*, 2024.

Peter Kairouz, Sewoong Oh, and Pramod Viswanath. The composition theorem for differential privacy. In *International conference on machine learning*, pages 1376–1385. PMLR, 2015.

Antti Koskela, Joonas Jälkö, and Antti Honkela. Computing tight differential privacy guarantees using fft. In *International Conference on Artificial Intelligence and Statistics*, pages 2560–2569. PMLR, 2020.

A. Krizhevsky. Learning multiple layers of features from tiny images. Technical report, University of Toronto, 2009. URL <https://www.cs.utoronto.ca/~kriz/learning-features-2009-TR.pdf>.

Y. LeCun, C. Cortez, and C. C. Burges. The mnist database of handwritten digits, 1998. URL <http://yann.lecun.com/exdb/mnist/>.

Samuel Maddock, Alexandre Sablayrolles, and Pierre Stock. Canife: Crafting canaries for empirical privacy measurement in federated learning. *arXiv preprint arXiv:2210.02912*, 2022.

Saeed Mahloujifar, Luca Melis, and Kamalika Chaudhuri. Auditing  $f$ -differential privacy in one run. *arXiv preprint arXiv:2410.22235*, 2024.

Ilya Mironov. Rényi differential privacy. In *2017 IEEE 30th computer security foundations symposium (CSF)*, pages 263–275. IEEE, 2017.

Milad Nasr, Shuang Songi, Abhradeep Thakurta, Nicolas Papernot, and Nicholas Carlini. Adversary instantiation: Lower bounds for differentially private machine learning. In *2021 IEEE Symposium on security and privacy (SP)*, pages 866–882. IEEE, 2021.

Milad Nasr, Jamie Hayes, Thomas Steinke, Borja Balle, Florian Tramèr, Matthew Jagielski, Nicholas Carlini, and Andreas Terzis. Tight auditing of differentially private machine learning. In *32nd USENIX Security Symposium (USENIX Security 23)*, pages 1631–1648, 2023.

Nicolas Papernot, Martín Abadi, Ulfar Erlingsson, Ian Goodfellow, and Kunal Talwar. Semi-supervised knowledge transfer for deep learning from private training data. *arXiv preprint arXiv:1610.05755*, 2016.

Reza Shokri, Marco Stronati, Congzheng Song, and Vitaly Shmatikov. Membership inference attacks against machine learning models. In *2017 IEEE symposium on security and privacy (SP)*, pages 3–18. IEEE, 2017.

Theresa Stadler, Bristena Oprisanu, and Carmela Troncoso. Synthetic data–anonymisation groundhog day. In *31st USENIX Security Symposium (USENIX Security 22)*, pages 1451–1468, 2022.

Thomas Steinke, Milad Nasr, Arun Ganesh, Borja Balle, Christopher A Choquette-Choo, Matthew Jagielski, Jamie Hayes, Abhradeep Guha Thakurta, Adam Smith, and Andreas Terzis. The last iterate advantage: Empirical auditing and principled heuristic analysis of differentially private sgd. *arXiv preprint arXiv:2410.06186*, 2024a.

Thomas Steinke, Milad Nasr, and Matthew Jagielski. Privacy auditing with one (1) training run. *Advances in Neural Information Processing Systems*, 36, 2024b.

Pratiksha Thaker, Shengyuan Hu, Neil Kale, Yash Maurya, Zhiwei Steven Wu, and Virginia Smith. Position: Llm unlearning benchmarks are weak measures of progress. *arXiv preprint arXiv:2410.02879*, 2024.

Florian Tramer, Andreas Terzis, Thomas Steinke, Shuang Song, Matthew Jagielski, and Nicholas Carlini. Debugging differential privacy: A case study for privacy auditing. *arXiv preprint arXiv:2202.12219*, 2022.

Jiayuan Ye and Reza Shokri. Differentially private learning needs hidden state (or much faster convergence). *Advances in Neural Information Processing Systems*, 35:703–715, 2022.

Samuel Yeom, Irene Giacomelli, Matt Fredrikson, and Somesh Jha. Privacy risk in machine learning: Analyzing the connection to overfitting. In *2018 IEEE 31st computer security foundations symposium (CSF)*, pages 268–282. IEEE, 2018.

Ashkan Yousefpour, Igor Shilov, Alexandre Sablayrolles, Davide Testuggine, Karthik Prasad, Mani Malek, John Nguyen, Sayan Ghosh, Akash Bharadwaj, Jessica Zhao, et al. Opacus: User-friendly differential privacy library in pytorch. *arXiv preprint arXiv:2109.12298*, 2021.

Santiago Zanella-Beguelin, Lukas Wutschitz, Shruti Tople, Ahmed Salem, Victor Rühle, Andrew Paverd, Mohammad Naseri, Boris Köpf, and Daniel Jones. Bayesian estimation of differential privacy. In *International Conference on Machine Learning*, pages 40624–40636. PMLR, 2023.

Yuqing Zhu, Xiang Yu, Manmohan Chandraker, and Yu-Xiang Wang. Private-knn: Practical differential privacy for computer vision. In *Proceedings of the IEEE/CVF Conference on Computer Vision and Pattern Recognition*, pages 11854–11862, 2020.